Immobilization of the heteropoly acid (HPA) $H_4SiW_{12}O_{40}$ (SiW_{12}) on mesoporous molecular sieves (HMS and MCM-41) and their catalytic behavior

Wenling Chu, Xiangguang Yang, Yongkui Shan, Xingkai Ye and Yue Wu [1]

Changchun Institute of Applied Chemistry, Chinese Academy of Sciences, Changchun, Jilin 130022, PR China

Received 11 July 1996; accepted 18 September 1996

Supported catalysts, consisting of SiW_{12} immobilized on hexagonal mesoporous silica (HMS) and its aluminum-substituted derivative (MCM-41) with different loadings and calcination temperatures, have been prepared and characterized by X-ray diffraction, FT-IR and NH_3-temperature programmed desorption. It is shown that SiW_{12} retains the Keggin structure on the mesoporous molecular sieves and no HPA crystal phase is developed, even at SiW_{12} loadings as high as 50 wt%. In the esterification of acetic acid by *n*-butanol, supported catalysts exhibit a higher catalytic activity and stability and held some promise of practical application. In addition, experimental results indicate that the loaded amount of SiW_{12} and the calcination temperatures have a significant influence on the catalytic activity, and the existence of aluminum has also an effect on the properties of supported catalysts.

Keywords: heteropoly acid; mesoporous molecular sieves; esterification

1. Introduction

MCM-41 is a novel mesoporous molecular sieve invented in the Central Research Laboratory of The Mobil Research and Development Cooperation [1]. High thermal stability (up to 1198 K), larger surface area (over 700 m^2/g) and adsorption capacity for aromatic organic molecules render this material very interesting for catalysis [2] and support [3,4].

Using dodecylamine (DDA) as a template replacing the conventional quaternary, ammonium ion surfactant, Tanev et al. [5] prepared the hexagonal mesoporous silicas (HMS) at ambient temperature. As MCM-41, HMS was also characterized by a single X-ray diffraction peak corresponding to a *d*-spacing of about 37.7 Å. An advantage of the pure-silica HMS with respect to the MCM-41 phase was that it could be prepared at ambient temperature, without the help of an autoclave. In addition, HMS typically has a surface area above 700 m^2/g with a large pore volume. Pure-silica HMS can be heated to at least 800°C without its structural collapse [6]. Due to these properties, HMS would be an excellent support for the loading of HPAs.

Heteropoly acids (HPAs) are a new type of multifunctional catalytic materials. Regardless of whether they exist in aqueous or nonaqueous solutions, HPAs are very strong Brønsted acids, of which the acid strength is even higher than that of mineral acids used in industry [7,8]. Thus they have been used successfully in acidic reactions such as esterification [9]. Unfortunately, since they are highly soluble in polar media, they are often difficult to separate from the reaction products, which is problematic in industrial processes. Therefore, numerous investigations of supported catalysts in fundamental research have attracted increasing attention worldwide [10]. It appears that, as an inert support, pore dimensions of MCM-41 and HMS can be engineered in the range from 15 to 100 Å, which allow the easy introduction of HPA molecules (~ 12 Å diameter) into the pores of the support. It is important for supported catalysts to realize heterogenization of homogeneous reactions.

We report here the results on the esterification of acetic acid by *n*-butanol catalyzed by a supported heteropoly acid with different loadings and calcination temperatures. The heteropoly acid chosen for these studies was $H_4SiW_{12}O_{40}$ (denoted as SiW_{12} in the text). The vapor-phase esterification was performed in a fixed-bed flow reactor.

2. Experimental

2.1. Materials

Preparation of the HMS support. The hexagonal mesoporous silica (HMS) was prepared by adding a clear solution of $Si(OC_2H_5)_4$ (1.00 mol) in ethanol (6.54 mol) to a stirred solution of dodecylamine (0.27 mol) and HCl (0.02 mol) in water (36.3 mol). Allowing the resulting gel to age for 18 h at room temperature afforded the crystalline templated product. The as-synthesized product was then calcined at 923 K for 5 h in air to remove the structurally incorporated template.

[1] To whom correspondence should be addressed.

Preparation of the MCM-41 support. A first solution (solution A) was prepared by mixing NaOH (1.0 g), $Al(NO_3)_2$ (1.9 g) and distilled water (40 ml). A second solution (B) contained $C_{16}H_{33}(CH_3)_3NBr$ (5.0 g), NaOH (1.0 g) and distilled water (50 ml). Solution A was added slowly to solution B under vigorous stirring. Stirring was maintained for about 30 min, and 20 g of silica gel (40% SiO_2) was added under stirring for the other 30 min. Then, this mixture was placed in a static autoclave at 160°C for 72 h. After cooling to room temperature, the resulting solid product was recovered by filtration on a Buchner funnel, washed with water and dried in air at ambient temperature. The resulting solid product was recovered and processed to a calcined form using the method described above.

Preparation of supported catalysts. A heteropoly acid named dodecatungstosilicic acid (SiW_{12}) was prepared as reported in the literature [11]. The catalysts were obtained by shaking a SiW_{12} aqueous solution (10 ml, 0.01–0.1 g HPA/ml) with HMS and MCM-41, respectively. The products were slowly dried under heating. The supported catalysts with different loadings were calcined at 373, 473 and 573 K. These calcined samples are hereafter referred to as sample (K1), sample (K2) and sample (K3), respectively.

All chemical reagents used were analytical grade.

2.2. Techniques

X-ray diffraction (XRD) measurements were carried out on a Rigaku D/max-qB diffractometer using Cu Kα radiation.

FT-IR spectra were recorded on a Bio-Rad spectrometer in KBr pellets over the range of 400–4000 cm^{-1} under atmospheric conditions.

NH_3-temperature programmed desorption (NH_3-TPD) was done in a home-made apparatus. The supported samples (100 mg) were treated in a helium stream at 723 K for 1 h and cooled to room temperature in the same atmosphere. NH_3 was adsorbed at 323 K for 1 h and then swept with helium as carrier gas until the chromatogram was stable. Desorption was carried out at a heating rate of 20 K/min.

2.3. Reaction

The esterification of acetic acid with *n*-butanol was carried out in a fixed-bed flow reactor with 15 mm internal diameter and 200 mm length at atmospheric pressure. The supported catalyst was placed at the center of the reactor and covered with a preheating zone of quartz sand. The experimental conditions were as follows: molar ratio of *n*-butanol to acetic acid is 1.0, weight hourly space velocity (WHSV) is 6 h^{-1} and the mass of catalyst used is 1.0 g.

The products were analyzed by a gas chromatograph (a column containing di-*n*-nontylsebacate) supplied with a thermal conductivity detector. Hydrogen was employed as the carrier gas.

3. Results and discussion

3.1. Characterization of mesoporous molecular sieves and supported catalyst

3.1.1. X-ray diffraction patterns

Fig. 1 shows the XRD patterns for the original HMS and MCM-41. The HMS exhibits a very strong peak at a *d*-spacing of 37.7 Å, which is in agreement with the literature [12]. It can be noted that a single diffraction peak occurs at a *d*-spacing of 37.7 Å for the pure silica HMS but at a *d*-spacing of 45.9 Å for MCM-41 containing Al. Intense low-angle reflections are characteristic of MCM-41 containing aluminum, but owing to the long-range hexagonal order, the weaker 110, 200 and 210 reflections might be observed in the 2θ range from 3.0 to 7.0, and the appearance of 3–4 peaks which can be indexed on a hexagonal lattice is typical of MCM-41 materials.

The experimental results show that the X-ray powder diffraction patterns for SiW_{12}/HMS samples (figures were omitted) and SiW_{12}/MCM-41 samples (fig. 2) are nearly identical. As expected, the intensity of the peak at 45.9 Å decreases when SiW_{12} was immobilized on MCM-41, and no low-range reflections were observed at 50 wt% loadings which indicated that, at higher load-

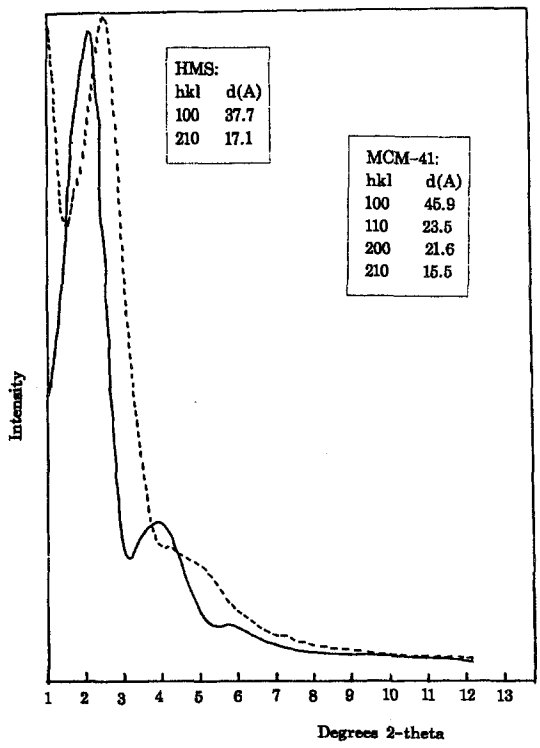

Fig. 1. X-ray powder diffraction patterns of initial MCM-41 (——) and HMS (- - -).

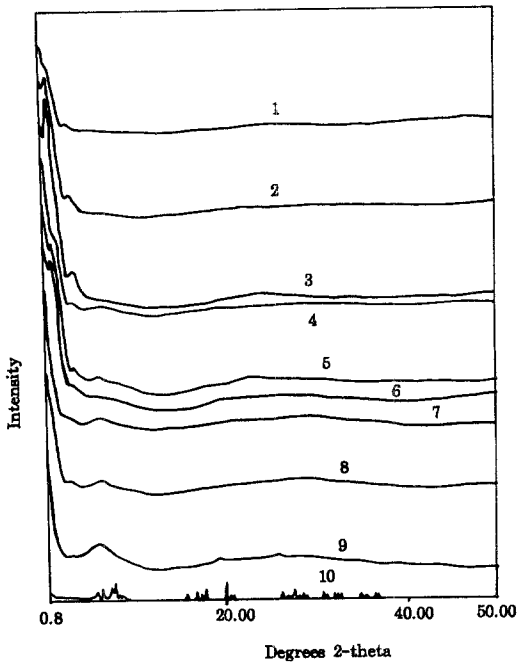

Fig. 2. X-ray powder diffraction patterns of various SiW_{12}/MCM-41 samples. (1) 10 wt%, SiW_{12}/MCM-41 (100°C); (2) 10 wt%, SiW_{12}/MCM-41 (200°C); (3) 10 wt%, SiW_{12}/MCM-41 (300°C); (4) 30 wt%, SiW_{12}/MCM-41 (100°C); (5) 30 wt%, SiW_{12}/MCM-41 (200°C); (6) 30 wt%, SiW_{12}/MCM-41 (300°C); (7) 50 wt%, SiW_{12}/MCM-41 (100°C); (8) 50 wt%, SiW_{12}/MCM-41 (200°C); (9) 50 wt%, SiW_{12}/MCM-41 (300°C); (10) SiW_{12}.

ings, the stacking of SiW_{12} on themselves can block the pores of MCM-41. For samples with the same loadings, with the calcination temperature increasing from 373 to 573 K, the intensity of the diffraction peak tends to increase. The reason is probably that calcination removes the templating molecules from the pores and renders the samples orderly arrayed. Moreover, for samples with various loadings and calcination temperatures, no SiW_{12} crystallinity was observed, even at an SiW_{12} loading as high as 50 wt%. This result can be explained by the large surface area of the support (above 700 m^2/g) and the easy access of HPA molecules (~ 12 Å diameter) to the mesopores of the support (30–50 Å). Assuming the cross-sectional area of the HPA molecule to be equal to 100 $Å^2$, one can calculate that, at 50 wt% SiW_{12} loading, HPA occupies at most 1/6 of the total surface area of mesoporous molecular sieves. In contrast, when HPA is loaded on an amorphous silica (S_{BET} = 200–300 m^2/g), the HPA crystallinity already appears at 20 wt% HPA content [13–15]. When compared on a per surface area basis, we found that the appearance of crystallites occurred at 70 wt% loading on MCM-41, which is the same HPA load/m^2 as 20 wt% on conventional silica.

3.1.2. FT-IR spectra

Infrared spectroscopic features of the framework vibrations of original HMS and MCM-41 are shown in fig. 3. For original HMS and MCM-41, the intrinsic vibrations of the TO_4 (T = Al or Si) tetrahedra are supposed to be structure insensitive. According to Flanigen et al. [16], they give "internal" bands at about 1100, 800 and 450 cm^{-1}. However, we notice an effect of dealumination: the band at 1078 cm^{-1} for MCM-41 was shifted by 11 cm^{-1} to the higher frequency of the pure silica HMS of 1089.2 cm^{-1}. A broad band at about 3500 cm^{-1}, which is best seen from fig. 3, corresponds to internal silanols. Considering the structure of MCM-41, one could infer that the internal silanols reside on the framework defects. Compared to the HMS, due to more defects derived from the Al, the band of the internal sila-

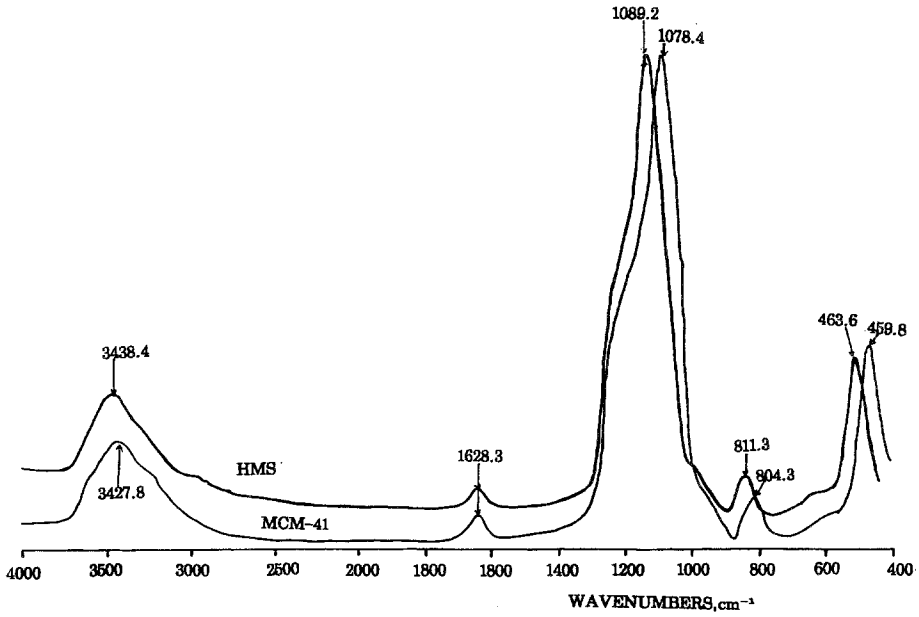

Fig. 3. Infrared spectrum of the initial material HMS and MCM-41.

nols was shifted. In addition, there is a template band at 1628.3 cm^{-1}, which is the bending vibration of NH, which may indicate that the template is not completely removed even after 5 h at such a high temperature as 923 K. The spectra of the supported samples are also identical. For example, the spectra of SiW_{12}/HMS (fig. 4) show that the SiW_{12} Keggin structure is retained in these samples. But for low SiW_{12} content, the characteristic band intensity of the heteropoly anion decreased. This can be explained by the fact that the direct interaction between intact SiW_{12} and the HMS surface weakens the interaction between bands in the heteropoly anion. Compared to the spectrum of bulk SiW_{12}, it is seen that the bands for W=O show small 4 cm^{-1} blue shifts and the bands for edge-bridging W–O–W show about 13 cm^{-1} red shifts, probably due to interaction between the SiW_{12} anion and the HMS surface. However, there are no obvious differences among the samples obtained at various calcination temperatures.

3.1.3. NH_3-temperature programmed desorption

The TPD graphs of original HMS and MCM-41 show two distinct peaks at 380 K and about 680 K for HMS and a peak at 430 K for MCM-41. The SiW_{12}/HMS samples have a large number of adsorption sites for NH_3 in the range of 373–573 K (fig. 5), the same as the SiW_{12}/MCM-41 samples (fig. 6). It is clear that the increase in the number of the adsorptive sites for NH_3 in this case either can be attributed to the acidic sites of SiW_{12} or is caused by the interaction of SiW_{12} with the surface of the support. The former can be formed after dehydration of SiW_{12}. This can be found by the appearance of a new NH_3-TPD desorption peak at about 573 K for sample (K2) and sample (K3). The reason is that calcination at higher temperature would strengthen the interaction between SiW_{12} and the support surface. On the other hand, the fact that dehydration of SiW_{12} treated at higher temperature makes protons easily movable is favorable to increase the acid strength of supported samples. Especially, when supported samples were calcined at 473 K, the peak (440 K) is higher than that of samples (K1). It is probable that calcination is favorable to strengthen the interaction between HPA and the surface of the support, which increases the number of active sites on the surface of supported catalysts. Furthermore, the fact based on the NH_3 desorption profile also proved the existence of this interaction for samples (K2). But, for the sample (K3) calcined at higher temperature, although its acid strength is the same as that of sample (K2), the number of active sites is smaller, even less than that of sample (K1). The reason may be that the calcination at higher temperature (300°C) could lead to partial destruction of some active sites in the catalyst.

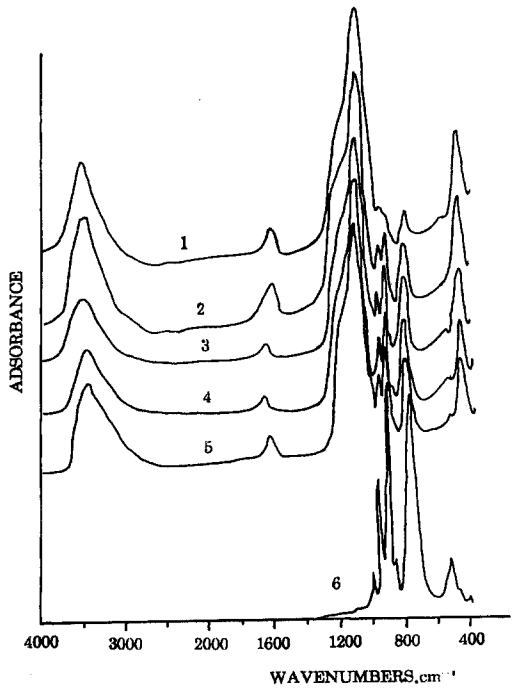

Fig. 4. Infrared spectrum of the various SiW_{12}/HMS samples. (1) 10 wt%, SiW_{12}/HMS (100°C); (2) 30 wt%, SiW_{12}/HMS (100°C); (3) 50 wt%, SiW_{12}/HMS (100°C); (4) 50 wt%, SiW_{12}/HMS (200°C); (5) 50 wt%, SiW_{12}/HMS (300°C); (6) SiW_{12}.

When comparing the NH_3-TPD graphs of figs. 5 and 6, it is noteworthy that, for samples (K1) with the same loading, the acid strength of the SiW_{12}/MCM-41 sample is higher than that of SiW_{12}/HMS. A possible explanation can be the existence of framework aluminum species in MCM-41. Their nature and distribution depend on the initial composition (especially the Si/Al molar ratio) and structure of the zeolite [17]. Currently, no comprehensive view can be given concerning the chemical nature of the species. Kuhl [18] proposed that the framework aluminum species in zeolite are present in a cationic form, i.e., AlO^+; whether or not hexacoordinated, these species would give rise to Brønsted acidity directly according to

$$AlO^+ + H_2O \rightleftharpoons AlO(OH) + H^+ \quad (1)$$

or indirectly by enhancing the Brønsted acidity of other acid sites.

In addition, quantitative results obtained by Corma [19] for the pyridine adsorption show that the total acidity increased with the Al content and so does the fraction of strong Brønsted sites.

3.2. The catalytic activity of catalysts in esterification

The results of the catalytic behavior of SiW_{12}/HMS and SiW_{12}/MCM-41 at different temperatures from 110 to 150°C are listed in table 1. HMS itself has a lower activity of only 5.6–14.2% of esterification. However, SiW_{12}/HMS has an excellent catalytic activity for esterification. The coincidence of the high activity of SiW_{12}/HMS with the NH_3-TPD results indicates that SiW_{12} must be responsible for the acid catalytic activity of the catalyst. The catalytic activity of SiW_{12}/HMS increases

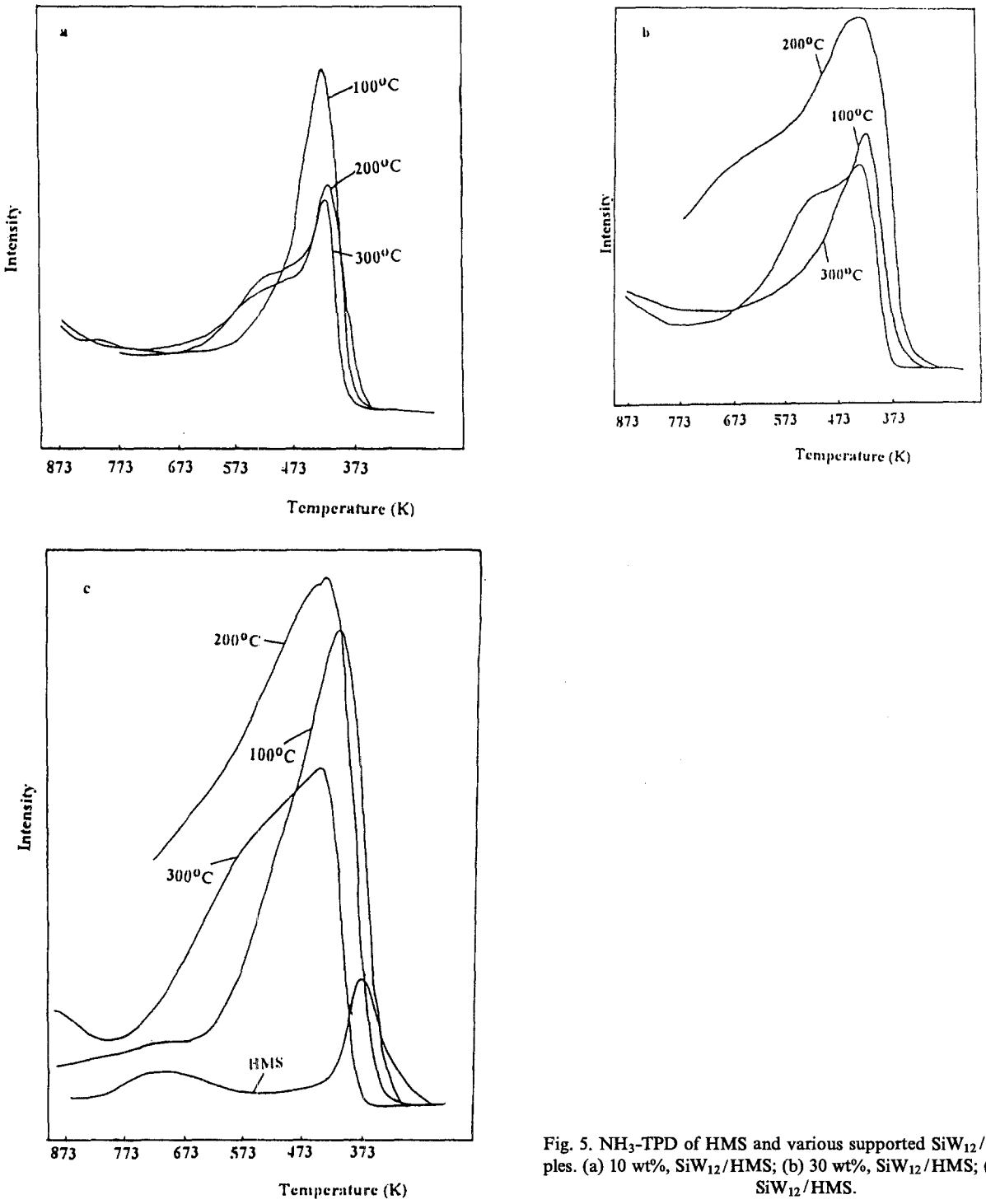

Fig. 5. NH_3-TPD of HMS and various supported SiW_{12}/HMS samples. (a) 10 wt%, SiW_{12}/HMS; (b) 30 wt%, SiW_{12}/HMS; (c) 50 wt%, SiW_{12}/HMS.

with increasing reaction temperature, which shows a significant difference when compared to that of SiW_{12}/carbon [20], namely, conversion of *n*-butanol dramatically increases above 130°C. This can be attributed to undesirable side reactions at high temperature. By gas chromatography, it can be found that, besides the formation of desirable *n*-butyl acetate, the SiW_{12}/HMS catalysts allow a considerable number of by-products to be obtained – 1-butene, 2-butene and *n*-butyl ether – at higher temperature. It is well known that the pore size of HMS (~ 30 Å) is greater than the average pore size of the activated carbon (~ 17 Å); the regularity of the pore system of HMS provides no advantage in selectivity for the smaller reactant in our reaction. But for organic compounds of large molecular size, it was reported in the literature [21,22] that, due to a significant steric hindrance, the uniformly sized mesoporous supported catalysts do show advantage in size and shape selectivity. But, surprisingly we noticed from our experimental results that SiW_{12}/MCM-41 catalysts have 100% selectivity to *n*-butyl acetate. Even at 150°C, no by-products were observed. This may be attributed, as stated above,

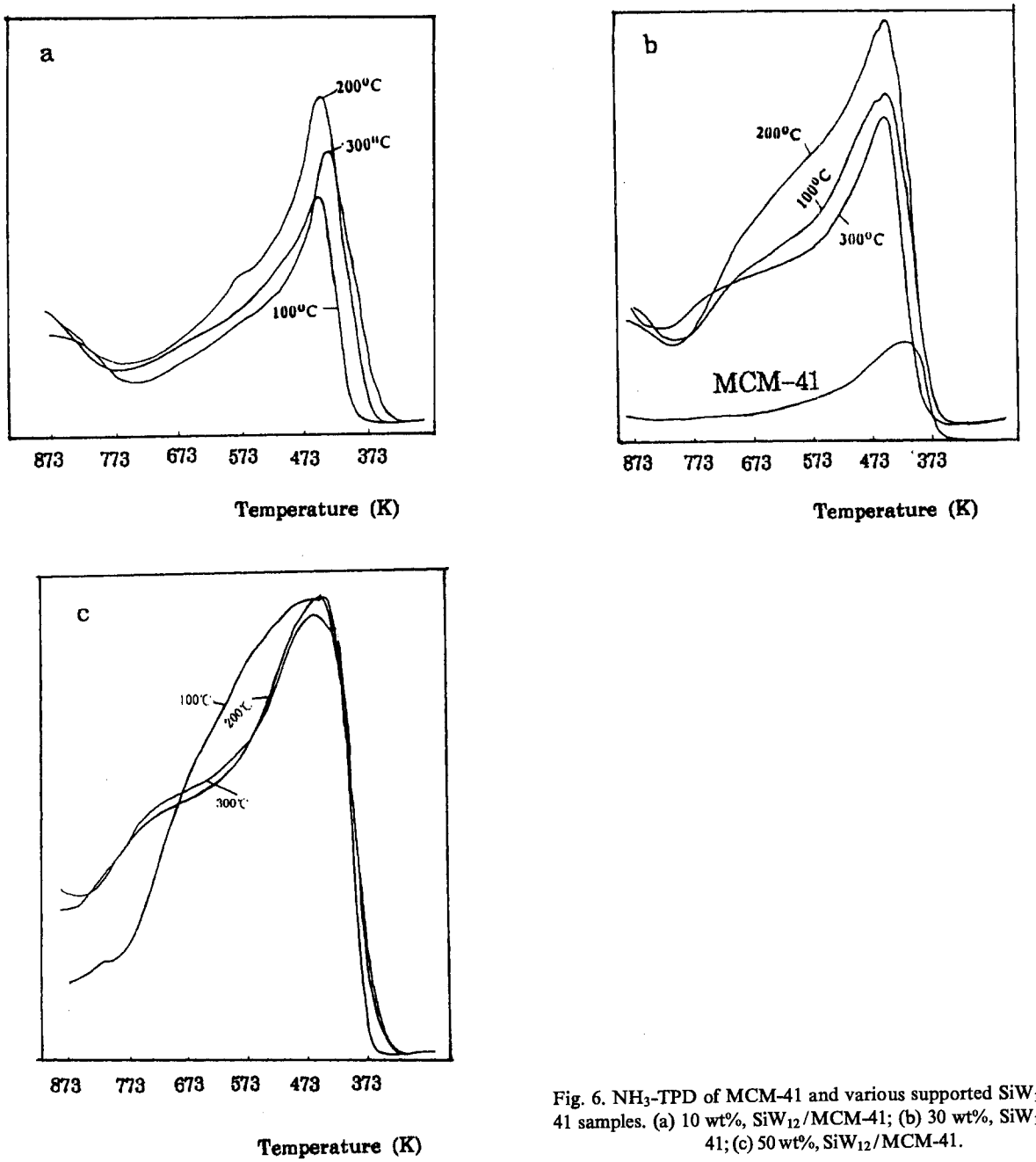

Fig. 6. NH_3-TPD of MCM-41 and various supported SiW_{12}/MCM-41 samples. (a) 10 wt%, SiW_{12}/MCM-41; (b) 30 wt%, SiW_{12}/MCM-41; (c) 50 wt%, SiW_{12}/MCM-41.

Table 1
Conversion (%) of *n*-butanol on various supported catalysts

Supported SiW_{12}/HMS	Reaction temperature (°C)					Supported SiW_{12}/MCM-41	Reaction temperature (°C)				
	110	120	130	140	150		110	120	130	140	150
10 wt%, 200°C	57.3	58.7	59.9	65.7	72.3	10 wt%, 200°C	28.1	33.0	33.9	34.9	39.3
30 wt%, 200°C	59.2	61.7	64.3	73.3	85.5	30 wt%, 200°C	46.5	49.0	51.2	53.9	73.5
50 wt%, 100°C	69.8	72.1	73.7	81.3	89.4	50 wt%, 100°C	59.0	72.0	75.8	78.1	81.9
50 wt%, 200°C	73.7	77.2	79.2	86.3	93.5	50 wt%, 200°C	68.9	71.2	76.6	81.2	86.5
50 wt%, 300°C	60.5	64.2	66.3	82.5	89.8	50 wt%, 300°C	–	65.9	67.4	73.5	79.6

Table 2
The amount of SiW_{12} eluted in gas–solid esterification (mg/g) and the surface area of supported samples

Supported catalyst	Preparation conditions	Surface area (m^2/g)	The amount of SiW_{12} eluted (mg/g)				
			110°C	120°C	130°C	140°C	150°C
SiW_{12}/HMS	50 wt%, 100°C	227.6	0.78	0.66	0.42	0.35	0.32
	50 wt%, 200°C	246.6	–	0.51	0.28	0.19	0.21
	50 wt%, 300°C	243.3	0.64	0.47	0.35	0.22	0.18
	30 wt%, 200°C	325.0	0.71	0.23	0.27	0.16	0.017
	10 wt%, 200°C	459.2	0.30	0.13	0.077	0.034	0.017
SiW_{12}/MCM-41	10 wt%, 100°C	570.9	–	0.30	0.19	0.14	0.12
	10 wt%, 200°C	609.1	–	0.16	0.18	0.042	0.042
	10 wt%, 300°C	557.6	–	0.28	0.25	0.21	0.11
	30 wt%, 100°C	368.8	–	0.75	0.42	0.12	0.068
	30 wt%, 200°C	365.0	0.69	0.20	0.094	0.077	0.077

to higher acid strength resulting from the existence of framework aluminum in MCM-41, which is so favorable to the process of esterification that the disadvantage of larger pores in selectivity for smaller reactants becomes insignificant. Generally speaking, the conversion of *n*-butanol catalyzed by sample (K2) is highest, which is in agreement with the results of NH_3-TPD. After calcination at higher temperature (200°C), the interaction of SiW_{12} and the support through the OH group and the protons becomes more stronger so that much SiW_{12} can get into the pores of the support, probably favoring the dispersion of the active sites in the case of sample (K2) and, consequently, increasing the number of active sites. In addition, it can be found from the data tabulated in table 2 that the surface area of the sample (50 wt%) slightly increases with calcination temperature, which may be due to the strong interaction of SiW_{12} and support at higher temperature.

For samples calcined at higher temperature, this stronger interaction between SiW_{12} and support appears to be further proved from the elution amount of HPA shown in table 2. The higher the calcination temperature of the sample, the lower the amount of HPA eluted out of the support. But it appears from our studies [20] that the firmness of SiW_{12} immobilized on supports studied in this paper is lower than that of the activated carbon as support. A reasonable explanation may be that this difference of immobilizing firmness is dependent on the surface chemical structure of the two kinds of supports [10]. It is known that there are many oxygen containing surface groups on the surface of activated carbon, which include not only the acidic groups of carboxyl, phenolic and lactonic groups, but also weaker basic C=O groups in favor of tightly immobilizing a certain amount of HPA through electrostatic attraction. In spite of washing with hot water or hot methanol by means of a Soxhlet extractor, entrapped catalysts with the maximum HPA content of 7.2–13.9 wt% were obtained [23].

Compared to activated carbon supports, there are fewer OH groups on the surface of mesoporous molecular sieves, which provides a weaker electrostatic attraction between SiW_{12} and surface OH groups. Even no adsorption of HPA could be observed in HPA aqueous solution at room temperature.

Furthermore, it can be found that the eluted amount of HPA decreases with decreasing loadings of SiW_{12}. This can be explained through the schematic model given in fig. 7.

The effect of loading on the eluted amount of SiW_{12} is consistent with the interaction between the SiW_{12} anions and protonated surface OH groups. This can be understood by considering that, during the impregnation, the protons of the strong Brønsted-acid SiW_{12} are transferred to the basic OH groups of the support surface. For high SiW_{12} loadings, free hydroxonium, H_3O^+, cations exist in the solution, favoring the deposit of SiW_{12} on the support. By contrast, for low SiW_{12} loadings, all hydrated H^+ from the 12-tungstosilicic acid tend to be fixed on the support surface. The surface becomes positively charged by the formation of $Si–OH_2^+$ groups

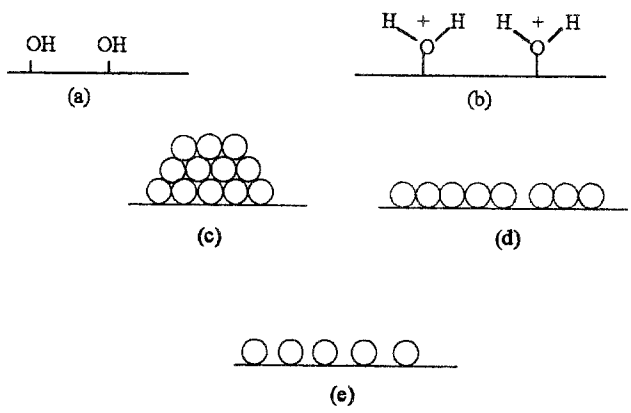

Fig. 7. Schematic model of the SiW_{12} anion on the HMS surface. (a) Surface with OH groups; (b) protonated surface hydroxyl group; (c) high coverage; (d) medium coverage; (e) low coverage.

which are able to strongly attract the naked SiW_{12} anions through electrostatic interaction (fig. 7e). This interpretation allows us to understand why the eluted amount of SiW_{12} decreases with decreasing SiW_{12} loadings.

References

[1] M.K. Rubin and P. Chu, US Patent 4 954 325 (1990).
[2] Pen-shin Eugene Dai, Catal. Today 26 (1995) 3.
[3] I.V. Kozhevnikov, A. Sinnema, R.J.J. Jansen, K. Pamin and H. van Bekkum, Catal. Lett. 30 (1995) 241.
[4] C. Liu, X. Ye and Y. Wu, Catal. Lett. 36 (1996) 263.
[5] P.T. Tanev, M. Chibwe and T.J. Pinnavaia, Nature 368 (1994) 321.
[6] C.-Y. Chen, H.-X. Li and M.E. Davis, Microporous Mater. 2 (1993) 17.
[7] Jozefowicz et al., Microporous Mater. 1 (1993) 313.
[8] I.V. Kozhevnikov and K.I. Matveer, Appl. Catal. 5 (1983) 135.
[9] M.A. Schwegler, H. van Bekkum and N.A. de Munck, Appl. Catal. 74 (1991) 191.
[10] Y. Wu, X.K. Ye, X.G. Yang, X.P. Wang, W.L. Chu and Y.H. Cai, Ind. Eng. Chem. Res. 35 (1996) 2546.
[11] G.A. Tsigdinos, Ind. Eng. Chem. Prod. Res. Develop. 13 (1974) 267.
[12] Y. Izumi, R. Hasebe and K. Urabe, J. Catal. 84 (1983) 402.
[13] K. Mohana Rao, P. Gobetto, A. Iannibello and A. Zecchina, J. Catal. 119 (1989) 512.
[14] S. Kasztelan, E. Payen and J.B. Moffat, J. Catal. 125 (1990) 45.
[15] Y. Izumi, R. Hasthe and K. Urabe, J. Catal. 84 (1983) 402.
[16] E.M. Flanigen, H. Khatami and H.A. Szymanski, Adv. Chem. Ser. 101 (1971) 201.
[17] J. Dwyer and P.J. O'Malley, Stud. Surf. Sci. Catal. 35 (1988) 5.
[18] G.H. Kuhl, J. Phys. Chem. Solids 38 (1977) 1259.
[19] A. Corma, C. Corell, V. Fornes, W. Kolodziejski and J. Pérez-Pariente, Zeolites 15 (1995) 576.
[20] W. Chu, X. Yang, X. Ye and Y. Wu, Appl. Catal., accepted.
[21] D.W. Breck, *Zeolite Molecular Sieves* (Wiley, New York, 1974).
[22] H. van Bekkum, E.M. Flanigen and J.C. Jansen, eds., *Introduction to Zeolite Science and Practice* (Elsevier, Amsterdam, 1991).
[23] Y. Izumi and K. Urabe, Chem. Lett. (1991) 663.